Formation of Chain and Large-Ring Polymeric Metal Complexes by the "Extended Reach" Sulfur Donor Ligands *N,N′*-Ethylenebis(pyrrolidine-2-thione) and *N,N′*-*p*-Phenylenedimethylenebis(pyrrolidine-2-thione)

Zeno Atherton, David M. L. Goodgame,* Stephan Menzer, and David J. Williams*

Chemistry Department, Imperial College of Science, Technology and Medicine, London SW7 2AY, U.K.

Received September 18, 1997

The preparations are reported of the "extended-reach" sulfur donor ligands *N,N′*-ethylenebis(pyrrolidine-2-thione) (EBPT) and *N,N′*-*p*-phenylenedimethylenebis(pyrrolidine-2-thione) (*p*-XBPT) and of a range of complexes with Co^{II}, Ni^{II}, Cu^{II}, Cu^{I}, Zn^{II}, Cd^{II}, and Ag^{I}, seven of which have been structurally characterized by X-ray crystallography. $[Co(NCS)_2(EBPT)]_n$ crystallizes in the orthorhombic space group $Pna2_1$, with $a = 10.339(4)$ Å, $b = 10.074(5)$ Å, $c = 16.832(7)$ Å, and $Z = 4$. $[ZnBr_2(EBPT)]_n$ crystallizes in the monoclinic space group $P2_1/n$, with $a = 9.979(4)$ Å, $b = 9.871(3)$ Å, $c = 16.057(6)$ Å, $\beta = 99.95(2)°$, and $Z = 8$. Both of these complexes contain tetrahedrally coordinated metal ions linked by EBPT bridges to form chains. $[CoCl_2(EBPT)]_2$ crystallizes in the tetragonal space group $I4_1/acd$, with $a = b = 14.400(1)$ Å, $c = 28.426(4)$ Å, and $Z = 16$. This compound forms discrete 18-membered rings. $[CuCl(EBPT)]_n$ crystallizes in the monoclinic space group $C2/c$, with $a = 19.188(3)$ Å, $b = 9.987(2)$ Å, $c = 15.964(3)$ Å, $\beta = 123.12(1)°$, and $Z = 8$. In this compound each EBPT ligand employs one monodentate S atom and one μ_2-S atom and forms ribbons of alternating $Cu_2(EBPT)_2$ 18-membered rings and four-membered $Cu_2(\mu_2\text{-}S)_2$ rings. $\{[CuBr(EBPT)]\cdot MeNO_2\}_n$ crystallizes in the monoclinic space group $C2/c$, with $a = 18.117(3)$ Å, $b = 9.932(1)$ Å, $c = 18.113(3)$ Å, $\beta = 90.70(1)°$, and $Z = 4$. This compound also has a ribbon structure, but here 18-membered $Cu_2(EBPT)_2$ rings alternate with Br-bridged Cu_2Br_2 units. $[Ni(NO_3)_2(p\text{-XBPT})]_n$ crystallizes in the monoclinic space group $C2/c$, with $a = 10.900(3)$ Å, $b = 14.474(4)$ Å, $c = 13.488(4)$ Å, $\beta = 99.24(2)°$, and $Z = 4$. The nickel atoms are bonded to two bidentate nitrates and two bridging *p*-XBPT ligands, forming chains. $\{[Co(p\text{-XBPT})_2](ClO_4)_2.4MeNO_2\}_n$ crystallizes in the monoclinic space group $C2/c$, with $a = 18.284(2)$ Å, $b = 17.897(3)$ Å, $c = 31.136(4)$ Å, $\beta = 102.38(1)°$, and $Z = 8$. Each Co is tetrahedrally coordinated to four sulfur atoms from four *p*-XBPT units which connect the metal centers into sheets of contiguous 52-membered rings. EBPT crystallizes in the monoclinic space group $P2_1/n$, with $a = 5.479(2)$ Å, $b = 9.560(4)$ Å, $c = 11.171(7)$ Å, $\beta = 95.79(2)°$, and $Z = 2$; the thiolactam rings are coplanar and the sulfur atoms anti-disposed. The role of ligand conformation in determining structural types is discussed.

Introduction

Recent interest in the design of metal complexes with network polymeric structures has been dominated by the use of nitrogen-donor ligands, and many examples have been described.[1] In terms of oxygen-donor ligands, frameworks formed by linking metal ions with carboxylate anions are also well-known,[2] and extended-reach neutral O donor ligands based on sulfoxide,[3] lactam,[4] and pyridone[5] donor groups have also been employed. In contrast, there is far less information on similar large-ring polymeric metal complexes formed by extended-reach sulfur-donor ligands.[6] This is surprising, given the well-known propensity for sulfide or thiolate anions to form cluster compounds by virtue of the μ_2- and μ_3-bridging ability of the sulfur atom, and also that a number of dithia-alkanes are known to form individual large metallacyclic rings.[7]

(1) Some lead-in references to the many known examples include the following: (a) Hoskins, B. F.; Robson, R.; Slizys, D. A. *J. Am. Chem. Soc.* **1997**, *119*, 2952. (b) Whiteford, J. A.; Lu, C. V.; Stang, P. J. *J. Am. Chem. Soc.* **1997**, *119*, 9, 2524. (c) Liu, J.; Paliwala, T.; Lim, S. C.; Yu, C.; Niu, T.; Jacobson, A. J. *Inorg. Chem.* **1997**, *36*, 923. (d) Blake, A. J.; Hill, S. J.; Hubbersty, P.; Li, W. S. *J. Chem. Soc., Dalton Trans.* **1997**, 913. (e) Hartshorn, C. M.; Steel, P. J. *Chem. Commun.* **1997**, 541. (f) Keller, S. W. *Angew. Chem., Int. Ed. Eng.* **1997**, *36*, 247. (g) Blake, A. J.; Champness, N. R.; Khlobystov, A. N.; Lemenovskii, D. A.; Li, W.-S.; Schroder, M. *Chem. Commun.* **1997**, 1339. (h) Losier, P.; Zaworotko, M. J. *Angew. Chem., Int. Ed. Eng.* **1996**, *35*, 2779. (i) Fujita, M.; Ogura, K. *Bull. Chem. Soc. Jpn.* **1996**, *69*, 1471.

(2) See, for example: (a) Yaghi, O. M.; Davis, C. E.; Li, G.; Li, H. *J. Am. Chem. Soc.* **1997**, *119*, 2861. (b) Chung, K. H.; Hong, E.; Do, Y.; Moon, C. H. *J. Chem. Soc., Dalton Trans.* **1996**, 3363. (c) Wei, P. R.; Wu, B. M.; Leung, W. P.; Mak, T. C. W. *Polyhedron* **1996**, *15*, 4041. (d) Gutschke, S. O. H.; Molinier, M.; Powell, A. K.; Winpenny, R. E. P.; Wood, P. T. *Chem. Commun.* **1996**, 823.

(3) Zhang, R. H.; Ma, B. Q.; Bu, X. H.; Wang, H. G.; Yao, X. K. *Polyhedron* **1997**, *16*, 1123.

(4) (a) Doyle, G. A.; Goodgame, D. M. L.; Hill, S. P. W.; Menzer, S.; Sinden, A.; Williams, D. J. *Inorg. Chem.* **1995**, *34*, 2850. (b) Goodgame, D. M. L.; Menzer, S.; Ross, A. T.; Williams, D. J. *Inorg. Chim. Acta* **1996**, *251*, 141.

(5) Goodgame, D. M. L.; Menzer, S.; Smith, A. M.; Williams, D. J. *Chem. Commun.* **1997**, 339 and references therein.

(6) (a) Atherton, Z.; Goodgame, D. M. L.; Katahira, D. A.; Menzer, S.; Williams, D. J. *J. Chem. Soc., Chem. Commun.* **1994**, 1423. (b) Goodgame, D. M. L.; Katahira, D. A.; Menzer, S.; Williams, D. J. *Inorg. Chim. Acta* **1995**, *229*, 77. (c) Munakata, M.; Wu, L. P.; Kuroda-Sowa, T.; Maekawa, M.; Suenaga, S.; Nakagawa, S. *J. Chem. Soc., Dalton Trans.* **1996**, 1525.

(7) e.g. (a) Errington, J.; McDonald, W. S.; Shaw, B. L. *J. Chem. Soc., Dalton Trans.* **1980**, 2309. (b) Stephan, D. W. *Organometallics* **1991**, *10*, 2037. (c) Huang, Y.; Drake, R. J.; Stephan, D. W. *Inorg. Chem.* **1993**, *32*, 3022.

S0020-1669(97)01180-4 CCC: $15.00
Published on Web 02/13/1998

As initial studies with the extended-reach ligands *N,N′*-ethylenebis(pyrrolidine-2-thione) (**I**, EBPT) and *N,N′*-ethylenebis(pyridin-2-thione) (**II**, EBPYT) gave examples of polymeric, large-ring complexes,[6a,b] we have explored a more extensive range of complexes with these ligands and also with *N,N′*-*p*-phenylenedimethylenebis(pyrrolidine-2-thione) (**III**, *p*-XBPT). We report here the results of the studies with **I** and **III**, including X-ray characterization of seven of the complexes which illustrate the range of structural types that can be obtained.

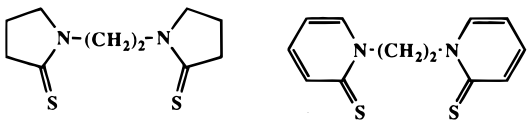

I

II

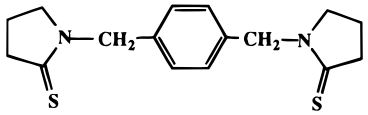

III

Experimental Section

Preparation of Compounds. CAUTION! *The preparation and use of these thione ligands was carried out in an efficient fume hood.*

***N,N′*-Ethylenebis(pyrrolidine-2-thione) (EBPT).** *N,N′*-Ethylenebis(pyrrolidine-2-one)[8] (6.1 g, 31.1 mmol) and Lawesson's reagent (12 g, 29.7 mmol) were refluxed in dry toluene (200 mL) under nitrogen for 7 h. The hot solution was decanted to remove some solid material, and the clear solution was then evaporated to dryness. The residue was refluxed with diethyl ether for 2 h, after which the solvent was decanted off and the solid residue dried in vacuo over P_2O_5. The resulting pale tan powder was recrystallized from water to yield pale tan crystals, which were dried in vacuo over P_2O_5 (51% yield). Mp: 145−147 °C. Anal. Calcd for $C_{10}H_{16}N_2S_2$: C, 52.6; H, 7.1; N, 12.3. Found: C, 52.4; H, 7.3; N, 12.0. EI-MS: *m/z* 228. ^{1}H NMR (270 MHz, $CDCl_3$, 298 K): δ 2.05 (4H, m, $CH_2CH_2CH_2$), 2.95 (4H, t, S=CCH_2CH$_2$), 3.95 (4H, t, NCH_2CH$_2$), 4.10 (4H, s, CH_2). The compound was also fully characterized by a single-crystal X-ray diffraction study (vide infra).

***N,N′*-*p*-Phenylenedimethylenebis(pyrrolidine-2-thione) (*p*-XBPT).** This was obtained from *N,N′*-*p*-phenylenedimethylenebis(pyrrolidine-2-one)[4b] by essentially the same method used for EBPT, but the product was purified by Soxhlet extraction with ethanol followed by recrystallization from warm nitromethane (50% yield). Mp: 207−208 °C. Anal. Calcd for $C_{16}H_{20}N_2S_2$: C, 63.1; H, 6.6; N, 9.2. Found: C, 62.9; H, 6.4; N, 9.2. EI-MS: *m/z* 304. ^{1}H NMR (270 MHz, $CDCl_3$, 298 K): δ 2.04 (4H, qn, $CH_2CH_2CH_2$), 3.10 (4H, t, S=CCH_2CH$_2$), 3.60 (4H, t, NCH_2CH$_2$), 4.98 (4H, s, CH_2), 7.31 (4H, s, aryl protons). The constitution of this ligand is also confirmed by the X-ray determinations of the structures of complexes **7** and **8** (vide infra).

Metal Complexes of EBPT. CAUTION! *Although we did not observe any explosive behavior with any of the perchlorate compounds described below, all metal perchlorates must be regarded as potentially explosive and appropriate safety measures must be taken (see, for example: J. Chem. Educ.* **1973**, *50*, A355).

$CoCl_2$(EBPT). A warm solution of $CoCl_2\cdot 6H_2O$ (0.065 mmol) in methanol (1 mL) was added to one of EBPT (0.026 mmol) in warm nitromethane (4 mL). To the clear blue solution was added 2,2-dimethoxypropane (2 mL) followed by 20 drops of methanol. A small amount of blue solid was removed by filtration, and after a further addition of 20 drops of methanol, the container was loosely covered and stored for 4 days, after which time small, turquoise-blue block crystals had formed (56% yield). Anal. Calcd for $C_{10}H_{16}Cl_2CoN_2S_2$: C, 33.5; H, 4.5; N, 7.8. Found: C, 33.6; H, 4.3; N, 7.9. ν(Co−Cl): 294 and 318 cm^{-1}. Electronic spectrum (reflectance): 5200sh, 6000, 7400, 14300sh, 15600, 16500sh cm^{-1}.

$[CoBr_2(EBPT)]_2\cdot 1.5MeOH$. 2,2-Dimethoxypropane (9 mL) was added to a solution containing $CoBr_2\cdot 6H_2O$ (0.22 mmol) and EBPT (0.22 mmol) in ethanol (9 mL). After warming for 10 min, the solution was stored over concentrated H_2SO_4 for ca. 5 h, during which time the product separated as blue blocks in essentially quantitative yield. Anal. Calcd for $C_{21.5}H_{38}Br_4Co_2N_4O_{1.5}S_4$: C, 27.4; H, 4.0; N, 6.0. Found: C, 27.6; H, 3.8; N, 5.7. ν(Co−Br): 224 and 258 cm^{-1}. Electronic spectrum (reflectance): 5100, 5900, 7300, 13900sh, 14600, 15400sh cm^{-1}.

$Co(NCS)_2$(EBPT). Slow concentration of a solution of cobalt(II) thiocyanate (0.2 mmol) and EBPT (0.2 mmol) in ethanol (8 mL) over concentrated H_2SO_4 gave dark blue block crystals in 62% yield. Anal. Calcd for $C_{12}H_{16}CoN_4S_4$: C, 35.7; H, 4.0; N, 13.9. Found: C, 35.7; H, 3.7; N, 13.8. ν(Co−NCS): 313 and 338 cm^{-1}. Electronic spectrum (reflectance): ca. 5200sh, 7600br, 14700sh, 15900, 16800sh cm^{-1}.

$Co(NO_3)_2$(EBPT). A solution of $Co(NO_3)_2\cdot 6H_2O$ (0.2 mmol) and EBPT (0.2 mmol) in a mixture of *n*-butanol (6 mL) and 2,2-dimethoxypropane (6 mL) was refluxed to give a purple solid, which was collected, washed with diethyl ether, and dried (72% yield). Anal. Calcd for $C_{10}H_{16}CoN_4O_6S_2$: C, 29.2; H, 3.9; N, 13.6. Found: C, 29.1; H, 3.9; N, 13.6.

$Co(ClO_4)_2$(EBPT)$_2\cdot H_2O$. CAUTION: *see warning above!* Slow concentration under reduced pressure of a solution of $Co(ClO_4)_2\cdot 6H_2O$ (0.13 mmol) and EBPT (0.26 mmol) in *n*-butanol (13 mL) gave turquoise, microcrystalline clumps of this complex in 27% yield. Anal. Calcd for $C_{20}H_{34}Cl_2CoN_4O_9S_4$: C, 32.8; H, 4.7; N, 7.7. Found: C, 32.9; H, 4.5; N, 7.5. Electronic spectrum (reflectance): 6900sh, 7600, 8300sh, 14100sh, 15200, 16700sh cm^{-1}.

Ni_2Cl_4(EBPT). A solution of $NiCl_2\cdot 6H_2O$ (0.2 mmol) and EBPT (0.2 mmol) in a mixture of *n*-butanol (6 mL) and 2,2-dimethoxypropane (6 mL) was refluxed to give a yellow solid, which was collected, washed with diethyl ether, and dried (92% yield). Anal. Calcd for $C_{10}H_{16}Cl_4Ni_2N_2S_2$: C, 24.6; H, 3.3; N, 5.8. Found: C, 24.4; H, 3.4; N, 5.5.

$NiBr_2$(EBPT). This bright green complex was obtained in 71% yield by the method used for the previous compound. Anal. Calcd for $C_{10}H_{16}Br_2NiN_2S_2$: C, 26.9; H, 3.6; N, 6.3. Found: C, 26.9; H, 3.5; N, 6.1. Electronic spectrum (reflectance): 5000br, 9100, 10000sh, 15400 cm^{-1}.

NiI_2(EBPT). A solution of nickel iodide (0.2 mmol) in ethanol (1 mL) was added to a hot solution of EBPT in a mixture of *n*-butanol (3 mL) and 2,2-dimethoxypropane (3 mL). Slow concentration of the resulting solution under reduced pressure gave a brown microcrystalline solid (55% yield). Anal. Calcd for $C_{10}H_{16}I_2NiN_2S_2$: C, 22.2; H, 3.0; N, 5.2. Found: C, 22.0; H, 2.7; N, 5.5. Electronic spectrum (reflectance): 5000br, 8300, 9600, 14000 cm^{-1}.

Ni(NCS)$_2$(EBPT). This greenish-yellow complex was obtained in very low yield (7%) by the method used for the previous compound, using an ethanolic solution of nickel thiocyanate prepared metathetically from hydrated nickel nitrate and sodium thiocyanate. Anal. Calcd for $C_{12}H_{16}NiN_4S_4$: C, 35.7; H, 4.0; N, 13.9. Found: C, 35.3; H, 3.6; N, 13.7.

$CuCl_2$(EBPT). Addition of a solution of EBPT (0.35 mmol) in a mixture of dichloromethane (5 mL) and nitromethane (5 mL) to one of $CuCl_2\cdot 2H_2O$ (0.17 mmol) in a mixture of methanol (0.2 mL) and nitromethane (1 mL) gave a deep purple precipitate of $CuCl_2$(EBPT). This was filtered off, washed with dichloromethane and dried over P_2O_5. Anal. Calcd for $C_{10}H_{16}Cl_2CuN_2S_2$: C, 33.1; H, 4.4; N, 7.7. Found: C, 32.9; H, 4.2; N, 7.5. ν(Cu−Cl): 313 and 325 cm^{-1}. X-band EPR spectrum: g_1, 2.04; g_2, 2.10; g_3, 2.19. Electronic spectrum (reflectance): 9300, 11800, 17900 cm^{-1}.

CuCl(EBPT). Slow evaporation of the filtrate from the above reaction gave bright yellow crystals of CuCl(EBPT). Anal. Calcd for $C_{10}H_{16}ClCuN_2S_2$: C, 36.7; H, 4.9; N, 8.6. Found: C, 36.5; H, 4.8; N, 8.6.

CuBr(EBPT)$\cdot$MeNO$_2$. A solution of copper(II) bromide (0.09 mmol) in methanol (0.7 mL) was added to a solution of EBPT (0.35 mmol) in nitromethane (5 mL). Brown-yellow block crystals formed

(8) Reppe, W. *Liebigs Ann. Chem.* **1955**, *596*, 1.

over a period of 7 days (68% yield). The compound was characterized by X-ray diffraction methods (see Results and Discussion).

$Cu(ClO_4)$(EBPT). CAUTION: *see warning above!* A solution of EBPT (0.35 mmol) in a mixture of dichloromethane (5 mL) and nitromethane (5 mL) was added to a solution of hydrated copper(II) perchlorate (0.11 mmol) in a mixture of methanol (0.2 mL) and nitromethane (1 mL). A transient green color was observed, and after gentle reflux, a yellow solid separated, which was collected, washed with nitromethane, and dried in vacuo (58% yield). Anal. Calcd for $C_{10}H_{16}ClCuN_2O_4S_2$: C, 30.7; H, 4.1; N, 7.2. Found: C, 30.7; H, 3.9; N, 7.3.

ZnX_2(EBPT) (X = Cl, Br). These compounds were prepared from the respective zinc salts by the same method as that used for the cobalt bromide complex. The *chloro* complex separated in 71% yield as microcrystalline "hemispheres". Anal. Calcd for $C_{10}H_{16}Cl_2N_2S_2Zn$: C, 32.9; H, 4.4; N, 7.7. Found: C, 33.1; H, 4.1; N, 7.6. ν(Zn−Cl): 294, 303 cm^{-1} (IR); 291, 306 cm^{-1}.(R). The *bromo* complex formed as clumps of needles (75% yield). Anal. Calcd for $C_{10}H_{16}Br_2N_2S_2Zn$: C, 26.5; H, 3.6; N, 6.2. Found: C, 26.8; H, 3.3; N, 6.1.

ZnI_2(EBPT): white powder from equimolar amounts of zinc iodide and EBPT in *n*-butanol (54% yield). Anal. Calcd for $C_{10}H_{16}I_2N_2S_2Zn$: C, 21.9; H, 3.0; N, 5.1. Found: C, 22.1; H, 2.7; N, 5.1.

$Zn(ClO_4)_2$(EBPT)$_2$·2H_2O. CAUTION: *see warning above!* Addition of an ethanolic solution of hydrated zinc perchlorate (0.13 mmol in 2 mL) to a hot solution of EBPT (0.26 mmol) in nitromethane (5 mL) gave a white solid, which was washed with diethyl ether (51% yield). Anal. Calcd for $C_{20}H_{36}Cl_2N_4O_{10}S_4Zn$: C, 31.7; H, 4.8; N, 7.4. Found: C, 31.8; H, 4.4; N, 7.5.

CdX_2(EBPT) (X = Cl, Br, I). These white compounds precipitated in virtually quantitative yields on mixing equimolar amounts of the respective cadmium halide and EBPT in ethanol.

Chloride. Anal. Calcd for $C_{10}H_{16}CdCl_2N_2S_2$: C, 29.2; H, 3.9; N, 6.8. Found: C, 29.3; H, 3.6; N, 6.8. ν(Cd−Cl): 256, 273 cm^{-1} (IR); 258 cm^{-1} (R).

Bromide. Anal. Calcd for $C_{10}H_{16}Br_2CdN_2S_2$: C, 24.0; H, 3.2; N, 5.6. Found: C, 24.0; H, 3.3; N, 5.6.

Iodide. Anal: Calcd for $C_{10}H_{16}CdI_2N_2S_2$: C, 20.2; H, 2.7; N, 4.7. Found: C, 20.3; H, 2.4; N, 4.5.

$Cd(NO_3)_2$(EBPT): white powder from equimolar amounts of hydrated cadmium nitrate and EBPT in *n*-butanol (75% yield). Anal. Calcd for $C_{10}H_{16}CdN_4O_6S_2$: C, 25.8; H, 3.5; N, 12.1. Found: C, 26.1; H, 3.1; N, 11.8.

$Cd(ClO_4)_2$(EBPT)$_2$. CAUTION: *see warning above!* A white precipitate resulted on mixing hot solutions of hydrated cadmium perchlorate (0.013 mmol) in ethanol (1 mL) and EBPT (0.26 mmol) in nitromethane (5 mL) (92% yield). Anal. Calcd for $C_{20}H_{32}Cl_2CdN_4O_8S_4$: C, 31.3; H, 4.2; N, 7.3. Found: C, 31.4; H, 4.0; N, 7.1.

Metal Complexes of *p*-XBPT. The synthetic methods used for these complexes were generally similar to those employed for the compounds with EBPT, so only brief details are given below.

CoX_2(*p*-XBPT) (X = Cl, Br, I, NCS): equimolar amounts of CoX_2 and *p*-XBPT in hot methanol/nitromethane.

Cl: blue, 71% yield. Anal. Calcd for $C_{16}H_{20}Cl_2CoN_2S_2$: C, 44.3; H, 4.6; N, 6.5. Found: C, 44.4; H, 4.4; N, 6.6. ν(Co−Cl): 303 and 330 cm^{-1}. Electronic spectrum (reflectance): 5600sh, 6000, 7800, 14400sh, 15100, 16000 cm^{-1}.

Br: blue, 51% yield. Anal. Calcd for $C_{16}H_{20}Br_2CoN_2S_2$: C, 36.7; H, 3.9; N, 5.4. Found: C, 36.7; H, 3.8; N, 5.6. Electronic spectrum (reflectance): 5300sh, 6100, 7600, 14200sh, 14700, 15500 cm^{-1}.

I: green, 15% yield. Anal. Calcd for $C_{16}H_{20}CoI_2N_2S_2$: C, 31.1; H, 3.3; N, 4.5. Found: C, 30.9; H, 3.1; N, 4.7. Electronic spectrum (reflectance): 5300sh, 6000, 7100, 13500sh, 14100, 15000sh cm^{-1}.

NCS: blue, 56% yield. Anal. Calcd for $C_{18}H_{20}CoN_4S_4$: C, 45.1; H, 4.2; N, 11.3. Found: C, 44.5; H, 4.1; N, 11.7. Electronic spectrum (reflectance): 5900sh, 7100, 8300, 15600, 16400sh, 16800sh cm^{-1}.

$Co(ClO_4)_2$(*p*-XBPT)$_2$. CAUTION: *see warning above!* Green material (58% yield) was obtained from hydrated cobalt(II) perchlorate and *p*-XBPT in a 3:1 mole ratio in methanol/nitromethane. Anal. Calcd for $C_{32}H_{40}Cl_2CoN_4O_8S_4$: C, 44.3; H, 4.7; N, 6.5. Found: C, 44.3; H, 4.9; N, 6.2. Electronic spectrum (reflectance): 5300, 6900, 8700sh, 14300sh, 14900, 16100 cm^{-1}.

NiX_2(*p*-XBPT) (X = Br, NO_3): equimolar amounts of NiX_2 and *p*-XBPT in hot methanol/nitromethane.

Br: dark green, 46% yield. Anal. Calcd for $C_{16}H_{20}Br_2N_2NiS_2$: C, 36.7; H, 3.9; N, 5.4. Found: C, 36.7; H, 3.7; N, 5.5. Electronic spectrum (reflectance): 5000br, 9300, 10200sh, 15000 cm^{-1}.

NO_3: green, 79% yield. Anal. Calcd for $C_{16}H_{20}N_4NiO_6S_2$: C, 39.4; H, 4.2; N, 11.5. Found: C, 39.2; H, 4.2; N, 11.3. Electronic spectrum (reflectance): 8500, 14700, 23300 cm^{-1}.

NiI_2(*p*-XBPT). A solution of nickel(II) iodide (0.26 mmol) in a mixture of methanol (0.3 mL) and nitromethane (1 mL) was added to *p*-XBPT in a mixture of nitromethane (5 mL) and dichloromethane (5 mL). After the brown solution was stirred for several minutes, a dark brown solid separated in 40% yield. Anal. Calcd for $C_{16}H_{20}I_2N_2NiS_2$: C, 31.1; H, 3.3; N, 4.5. Found: C, 31.4; H, 3.0; N, 4.6. Electronic spectrum (reflectance): 5000br, 8700sh, 9800, 14100 cm^{-1}.

CuX(*p*-XBPT)$_2$·CH_2Cl_2 (X = ClO_4, BF_4). CAUTION: *see warning above!* A solution of *p*-XBPT (0.26 mmol) in a mixture of nitromethane (5 mL) and dichloromethane (5 mL) was added dropwise to a stirred solution of the respective hydrated copper(II) salt (0.08 mmol) dissolved in a mixture of methanol (0.2 mL) and nitromethane (1 mL). In both reactions a transient green-brown color faded with the formation of a thick cream solid which, on refluxing the mixture, became yellow.

ClO_4: 67% yield. Anal. Calcd for $C_{33}H_{42}Cl_3CuN_4O_4S_4$: C, 46.3; H, 4.9; N, 6.5. Found: C, 45.9; H, 4.8; N, 6.9.

BF_4: 40% yield. Anal. Calcd for $C_{33}H_{42}BCl_2CuF_4N_4S_4$: C, 47.0; H, 5.0; N, 6.6. Found: C, 47.0; H, 4.9; N, 6.9.

ZnX_2(*p*-XBPT) (X = Cl, Br, I). These white compounds were prepared by the methods used for their cobalt(II) analogues.

Cl: 77% yield. Anal. Calcd for $C_{16}H_{20}Cl_2N_2S_2Zn$: C, 43.6; H, 4.6; N, 6.4. Found: C, 43.3; H, 4.5; N, 6.4. ν(Zn−Cl): 300, 316 cm^{-1} (IR); 301 cm^{-1} (R).

Br: 71% yield. Anal. Calcd for $C_{16}H_{20}Br_2N_2S_2Zn$: C, 36.3; H, 3.8; N, 5.3. Found: C, 36.5; H, 3.7; N, 5.4.

I: 64% yield. Anal. Calcd for $C_{16}H_{20}I_2N_2S_2Zn$: C, 30.8; H, 3.2; N, 4.5. Found: C, 30.7; H, 3.2; N, 4.6.

CdX_2(*p*-XBPT) (X = Cl, Br, I). These white compounds were prepared as for their EBT analogues, but using nitromethane as solvent for the *p*-XBPT.

Cl: 70% yield. Anal. Calcd for $C_{16}H_{20}CdCl_2N_2S_2$: C, 39.4; H, 4.1; N, 5.7. ν(Cd−Cl): 271 cm^{-1} (IR); 268 cm^{-1} (R). Found: C, 39.7; H, 4.1; N, 5.6.

Br: 69% yield. Anal. Calcd for $C_{16}H_{20}Br_2CdN_2S_2$: C, 33.3; H, 3.5; N, 4.9. Found: C, 33.7; H, 3.5; N, 5.4.

I: 86% yield. Anal. Calcd for $C_{16}H_{20}CdI_2N_2S_2$: C, 28.7; H, 3.0; N, 4.2. Found: C, 28.9; H, 2.8; N, 4.1.

$Ag_2(ClO_4)_2$(*p*-XBPT)$_3$·H_2O. CAUTION: *see warning above!* This cream-colored complex precipitated immediately on addition of a solution of *p*-XBPT (0.26 mmol) in a mixture of dichloromethane (5 mL) and nitromethane (5 mL) to a solution of silver(I) perchlorate monohydrate (0.13 mmol) in methanol (0.25 mL) (67% yield). Anal. Calcd for $C_{48}H_{62}Ag_2Cl_2O_9S_6$: C, 42.8; H, 4.6; N, 6.2. Found: C, 42.8; H, 4.3; N, 6.3.

$Ag_2(BF_4)_2$(*p*-XBPT)$_3$·H_2O. Addition of a solution of silver tetrafluoroborate (0.016 mmol) in ethanol (1 mL) to one of *p*-XBPT (0.32 mmol) in nitromethane (7 mL) gave a cream solid within a few minutes (65% yield). Anal. Calcd for $C_{48}H_{62}Ag_2B_2F_8OS_6$: C, 43.7; H, 4.7; N, 6.4. Found: C, 43.5; H, 4.6; N, 6.3.

Microanalyses and Spectroscopy. Elemental analyses were performed by the Microanalytical Chemistry Laboratory, Imperial College. Infrared spectra were recorded on either a Perkin-Elmer 1720 FT spectrometer or an ATI Mattson Research Series FT spectrometer as Nujol mulls using CsI plates. Raman spectra were obtained on powdered samples at room temperature using a Perkin-Elmer 1760X FT spectrometer with a 1700X FT Raman accessory (Spectron Nd:YAG laser, 1064-nm excitation). The UV−vis reflectance spectra were recorded on a Beckman DK2 spectrometer on powdered samples in the range 4000−30000 cm^{-1}. EPR spectra were measured at room temperature on a Varian E12 X-band (ca. 9.5-GHz) spectrometer using powdered samples. NMR spectra were recorded on a JEOL JNM-EX270 spectrometer.

Table 1. Crystallographic Data for EBPT (**1**), $[CoCl_2((EBPT)]_2$ (**2**), $[Co(NCS)_2((EBPT)]_n$ (**3**), $[ZnBr_2((EBPT)]_n$ (**4**), $[CuCl(EBPT)]_n$ (**5**), $\{[CuBr(EBPT)]\cdot MeNO_2\}_n$ (**6**), $[Ni(NO_3)_2(p\text{-}XBPT)]_n$ (**7**), and $\{[Co(p\text{-}XBPT)_2](ClO_4)_2\cdot 4MeNO_2\}_n$ (**8**)

	1	**2**	**3**	**4**	**5**	**6**	**7**	**8**
formula	$C_{10}H_{16}N_2S_2$	$C_{10}H_{16}Cl_2CoN_2S_2$	$C_{12}H_{16}CoN_4S_4$	$C_{10}H_{16}Br_2N_2S_2Zn$	$C_{10}H_{16}ClCuN_2S_2$	$C_{11}H_{19}BrCuN_3O_2S_2$	$C_{16}H_{20}N_4NiO_6S_2$	$C_{36}H_{52}Cl_2CoN_8O_{16}S_4$
fw	228.4	358.2	403.5	453.6	327.4	432.9	487.2	1110.9
space group	$P2_1/n$	$I4_1/acd$	$Pna2_1$	$P2_1/n$	$C2/c$	$C2/c$	$C2/c$	$C2/c$
a, Å	5.479(2)	14.400(1)	10.339(4)	9.979(4)	19.188(3)	18.117(3)	10.900(3)	18.284(2)
b, Å	9.560(4)	14.400(1)	10.074(5)	9.871(3)	9.987(2)	9.932(1)	14.474(4)	17.897(3)
c, Å	11.171(7)	28.426(4)	16.832(7)	16.057(6)	15.964(3)	18.113(3)	13.488(4)	31.136(4)
β, deg	95.79(2)			99.95(2)	123.12(1)	90.70(1)	99.24(2)	102.38(1)
V, Å^3	582.1(5)	5894.0(11)	1753.1(13)	1557.9(10)	2562.2(7)	3258.6(8)	2100.4(11)	9951(2)
Z	2	16	4	8	8	4	4	8
ρ_{calcd}, g cm^{-3}	1.303	1.615	1.529	1.934	1.697	1.765	1.541	1.483
λ, Å	1.541 78	0.717 03	0.717 03	0.717 03	0.717 03	0.717 03	1.541 78	0.717 03
μ, cm^{-1}	38.46	17.90	14.52	69.55	22.13	40.52	35.55	6.93
T, °C	20	20	20	20	20	20	20	20
R_1[a]	0.0469	0.0474	0.0656	0.0600	0.0322	0.0388	0.0558	0.0745
wR_2[b]	0.1314	0.1149	0.1845	0.1425	0.0969	0.0927	0.1716	0.1903

[a] $R_1 = \sum(|F_o| - |F_c|)/\sum|F_o|$. [b] $wR_2 = [\sum(w\ |F_o^2 - F_c^2\ |)/\sum w|F_o^2|^2]^{1/2}$.

Table 2. Selected Bond Lengths (Å) and Angles (deg) for **1**

S(1)−C(1)	1.652(3)	C(1)−N(5)	1.322(3)
C(1)−C(2)	1.506(3)	C(2)−C(3)	1.515(4)
C(3)−C(4)	1.518(4)	C(4)−N(5)	1.461(3)
N(5)−C(6)	1.451(3)	C(6)−C(6A)	1.519(5)
N(5)−C(1)−C(2)	107.7(2)	N(5)−C(1)−S(1)	126.6(2)
C(2)−C(1)−S(1)	125.7(2)	C(1)−C(2)−C(3)	104.9(2)
C(2)−C(3)−C(4)	104.2(2)	N(5)−C(4)−C(3)	102.7(2)
C(1)−N(5)−C(6)	124.1(2)	C(1)−N(5)−C(4)	114.7(2)
C(6)−N(5)−C(4)	120.8(2)	N(5)−C(6)−C(6A)	110.7(2)

Table 3. Selected Bond Lengths (Å) and Angles (deg) for **2**

Co−Cl(8)	2.243(1)	Co−S(1)	2.349(1)
Cl(8)−Co−Cl(8B)	118.17(8)	S(1)−Co−S(1B)	121.38(8)
Cl(8)−Co−S(1)	97.56(5)	Cl(8)−Co−S(1B)	111.80(5)
Co−S(1)−C(2)	109.8(2)		

Table 4. Selected Bond Lengths (Å) and Angles (deg) for **3**

Co(1)−N(1)	1.964(9)	Co(1)−N(2)	1.907(9)
Co(1)−S(3)	2.322(3)	Co(1)−S(4)	2.317(2)
N(1)−C(1)	1.161(12)	C(1)−S(1)	1.604(11)
N(2)−C(2)	1.156(11)	C(2)−S(2)	1.623(9)
N(1)−Co(1)−N(2)	108.1(4)	N(1)−Co(1)−S(3)	109.2(5)
N(1)−Co(1)−S(4)	109.2(4)	N(2)−Co(1)−S(3)	118.9(4)
N(2)−Co(1)−S(4)	105.3(4)	S(3)−Co(1)−S(4)	105.8(1)
Co(1)−N(1)−C(1)	167.2(13)	Co(1)−N(2)−C(2)	168.5(10)
Co(1)−S(3)−C(30)	114.8(3)	Co(1)−S(4)−C(40)	110.5(3)
N(1)−C(1)−S(1)	177.5(13)	N(2)−C(2)−S(2)	177.5(11)

Table 5. Selected Bond Lengths (Å) and Angles (deg) for **4**

Zn(1)−Br(1)	2.387(2)	Zn(1)−Br(2)	2.363(2)
Zn(1)−S(1)	2.390(2)	Zn(1)−S(2)	2.358(2)
Br(1)−Zn(1)−Br(2)	116.92(5)	S(1)−Zn(1)−S(2)	105.62(9)
Br(1)−Zn(1)−S(1)	100.90(8)	Br(1)−Zn(1)−S(2)	103.94(8)
Br(2)−Zn(1)−S(1)	106.47(8)	Br(2)−Zn(1)−S(2)	120.73(8)
Zn(1)−S(1)−C(10)	108.7(3)	Zn(1)−S(2)−C(20)	113.8(4)

Crystallographic Analyses. Crystal data for EBPT (**1**), $[CoCl_2(EBPT)]_2$ (**2**), $[Co(NCS)_2(EBPT)]_n$ (**3**), $[ZnBr_2(EBPT)]_n$ (**4**), $[CuCl(EBPT)]_n$ (**5**), $\{[CuBr(EBPT)]\cdot MeNO_2\}_n$ (**6**), $[Ni(NO_3)_2(p\text{-}XBPT)]_n$ (**7**), and $\{[Co(p\text{-}XBPT)_2](ClO_4)_2.4MeNO_2\}_n$ (**8**) and summaries of the crystallographic analyses are given in Table 1. The data were collected on a Siemens P4/PC diffractometer, using ω scans and graphite-monochromated Cu Kα radiation for **1** and **7** and Mo Kα radiation for **2**−**6** and **8**. The data were corrected for Lorentz and polarization factors and for absorption. Structures **2**, **3**, and **6** were solved by the heavy-atom method and the remainder by direct methods. All the non-hydrogen atoms were refined anisotropically except for the perchlorate groups in **8** which were disordered. The hydrogen atoms were placed in calculated positions, assigned isotropic thermal parameters $U(H) = 1.2U_{eq}(C)$, and allowed to ride on their parent carbon atoms. Refinements were by full-matrix least squares based on F^2.

Computations were carried out using the SHELXTL PC system version 5.03.[9] Selected bond lengths and angles are given in Tables 2-9.

Table 6. Selected Bond Lengths (Å) and Angles (deg) for **5**

Cu−Cl	2.280(1)	Cu−S(1)	2.309(1)
Cu−S(14B)	2.376(1)	Cu−S(14C)	2.593(1)
Cu−Cu(A)	3.006(1)		
Cl−Cu−S(1)	124.72(4)	Cl−Cu−S(14B)	102.01(4)
S(1)−Cu−S(14B)	116.49(4)	Cl−Cu−S(14C)	108.80(4)
S(1)−Cu−S(14C)	97.66(4)	S(14B)−Cu−S(14C)	105.69(3)
Cu−S(1)−C(2)	110.48(13)	Cu−S(14B)−Cu(A)	74.31(3)

Table 7. Selected Bond Lengths (Å) and Angles (deg) for **6**

Cu(1)−S(17)	2.296(1)	Cu(1)−Br(2)	2.567(1)
Cu(3)−S(4)	2.314(1)	Cu(3)−Br(2)	2.571(1)
Cu(1)−Cu(3)	2.901(1)		
S(17)−Cu(1)−S(17A)	123.89(7)	S(17)−Cu(1)−Br(2)	114.03(3)
Br(2)−Cu(1)−Br(2A)	111.37(4)	S(17)−Cu(1)−Br(2A)	97.07(3)
Cu(1)−Br(2)−Cu(3)	68.75(3)	S(4)−Cu(3)−S(4A)	123.86(7)
S(4)−Cu(3)−Br(2)	101.56(3)	S(4)−Cu(3)−Br(2A)	109.38(3)
Br(2)−Cu(3)−Br(2A)	111.13(4)	Cu(1)−S(17)−C(16)	110.4(2)
Cu(3)−S(4)−C(5)	107.5(2)		

Table 8. Selected Bond Lengths (Å) and Angles (deg) for **7**

Ni−O(13)	2.073(3)	Ni−O(14)	2.130(3)
Ni−S(2)	2.370(1)		
O(13)−Ni−O(13A)	157.7(2)	O(13)−Ni−O(14)	61.4(1)
O(13)−Ni−O(14A)	101.5(1)	O(14)−Ni−O(14A)	87.8(2)
O(13)−Ni−S(2A)	101.7(1)	O(13)−Ni−S(2)	93.8(1)
O(14)−Ni−S(2A)	162.7(1)	O(14)−Ni−S(2)	92.4(1)
S(2)−Ni−S(2A)	92.6(1)	Ni−S(2)−C(3)	108.6(2)
O(13)−N(12)−O(14)	115.1(4)		

Table 9. Selected Bond Lengths (Å) and Angles (deg) for **8**

Co−S(1)	2.308(3)	Co−S(20)	2.334(3)
Co−S(21)	2.337(3)	Co−S(40)	2.322(3)
S(1)−Co−S(20)	96.0(1)	S(1)−Co−S(21)	115.3(1)
S(1)−Co−S(40)	116.5(1)	S(20)−Co−S(40)	115.2(1)
S(21)−Co−S(40)	97.5(1)	S(20)−Co−S(21)	117.9(1)
Co−S(1)−C(2)	107.1(3)	Co−S(20)−C(19)	107.5(3)
Co−S(21)−C(22)	106.4(4)	Co−S(40)−C(39)	106.2(3)

(9) Sheldrick, G. M. SHELXTL Version 5.03, University of Göttingen, Germany, 1995.

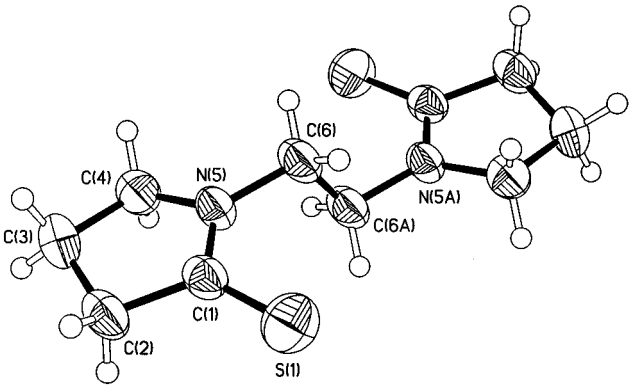

Figure 1. Molecular structure of EBPT (50% probability ellipsoids).

Results and Discussion

Ligands **I** and **III** can be readily prepared in reasonable yields (ca. 50%) by the action of Lawesson's reagent on their bis(lactam) analogues. They were characterized by conventional spectroscopic methods, but isolation of good crystals of **I** in the early stages of the work also permitted determination of its crystal structure, thus providing unambiguous confirmation of the nature of the compound and information about its geometry in the uncomplexed state.

Structure of *N,N′*-Ethylenebis(pyrrolidine-2-thione) (EBPT) 1. The X-ray study of **1** shows that, in the solid state, the molecule has C_i symmetry, resulting in an anti conformation of the two thiolactam units (Figure 1). The NCH_2CH_2N backbone is planar and oriented orthogonally (87°) to the planes of the two pyrrolidine-2-thione rings.

Metal Complexes. Our principal aim was to study the ability of these extended-reach sulfur donor ligands to form polymeric framework-type structures and to compare their behavior in this respect with that of their O-donor analogues. Accordingly, although we have explored their reactions with a range of metal salts (summarized in the Experimental Section), we discuss here mainly the definitive long-range structural information for a selection of the compounds, and some additional information about the metal ion coordination geometry, obtained by spectroscopic studies, for a number of the others.

Complexes of *N,N′*-Ethylenebis(pyrrolidine-2-thione). With the halides of Co^{II}, Ni^{II}, Zn, and Cd, EBPT generally gave complexes of stoichiometry MX_2(EBPT), though with nickel chloride the product isolated had the stoichiometry Ni_2Cl_4(EBPT). Complexes of type MX_2(EBPT) were also obtained with the thiocyanates of Co^{II} and Ni^{II}, and with the nitrates of Co^{II} and Cd, but with perchlorate as anion, the isolated products had 2:1 EBPT:M stoichiometry.

The main features of the structure of the blue complex $CoBr_2$(EBPT) have been given in a preliminary communication.[6a] In that compound two tetrahedral $CoBr_2S_2$ centers are linked by EBPT bridges to form a discrete 18-membered ring (Figure 2a). The dark blue complexes CoX_2(EBPT)(X = Cl, NCS) and the turquoise blue complex $Co(ClO_4)_2(EBPT)_2 \cdot H_2O$ also have solid-state electronic spectra characteristic[10] of an essentially tetrahedral coordination geometry about the metal ion, showing three strong, overlapping bands in the region 5000−9000 cm^{-1} [transitions to components of $^4T_1$(F)] and a strong multicomponent band centered on ca. 16 000 cm^{-1} [transitions to components of $^4T_1$(P)]. Furthermore, the low-frequency IR data [ν(Co−Cl), 294 and 318 cm^{-1}; ν(Co−NCS), 313 and 338 cm^{-1}] are also consistent[11] with this coordination geometry. These

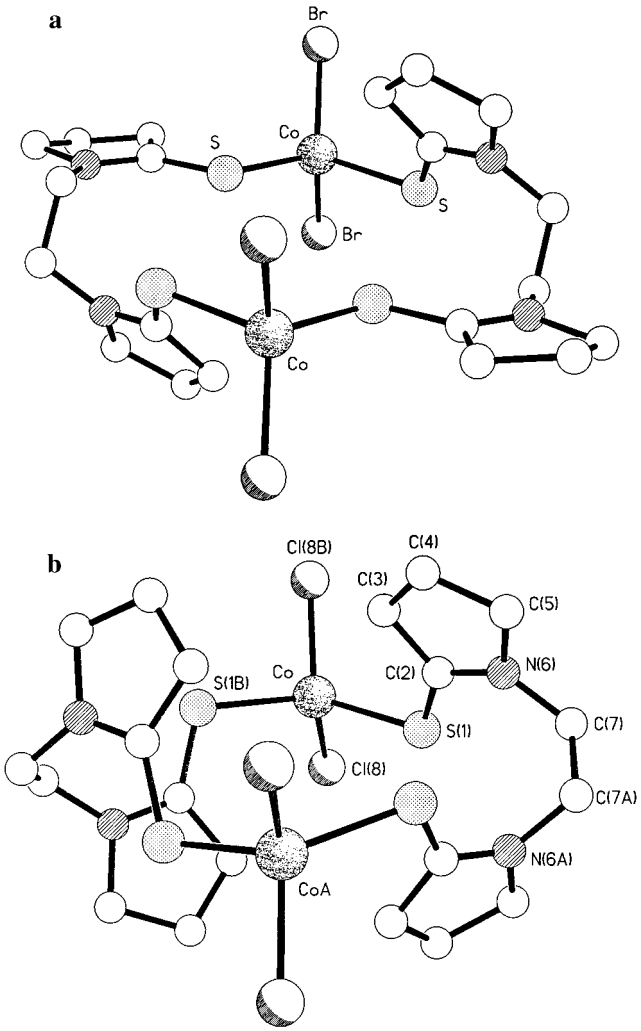

Figure 2. A comparison of the 18-membered ring structures formed by (a) $[CoBr_2(EBPT)]_2$[6a] and (b) $[CoCl_2(EBPT)]_2$.

conclusions about the primary coordination sphere have been confirmed by the X-ray studies, but the extended structures of $CoCl_2$(EBPT) and $Co(NCS)_2$(EBPT) are quite different.

Structure of $[CoCl_2(EBPT)]_2$ (2). The X-ray study of **2** reveals a structure that is similar to its bromide analogue (Figure 2a),[6a] in forming a discrete, dimeric, 18-membered ring in which two bridging EBPT ligands link two tetrahedrally coordinated cobalt(II) centers (Figure 2b). The coordination geometry about each cobalt atom is appreciably distorted with bond angles in the range 97.6(1)−121.4(8)° and Co−Cl and Co−S bond lengths of 2.243(1) and 2.349(1) Å respectively [cf. angles of 98.3(1)−114.3(1)° and a Co−S bond length of 2.319(3) Å for $CoBr_2$(EBPT)].

As in $CoBr_2$(EBPT), the bridging EBPT ligands have a gauche conformation about the NCH_2CH_2N spacer unit [$-CH_2-CH_2-$ torsion angle = 67°, cf. 68° in Co(EBPT)Br_2]. However, in **2** the EBPT ligand has crystallographic C_2 symmetry about an axis passing through the CH_2CH_2-group which results in an anti conformation for the two thiolactam units. This contrasts with the syn geometry observed in the analogous bromide and results in a marked difference in the conformations of the 18-membered macrocyclic rings in the two compounds. In the

(10) Goodgame, D. M. L.; Goodgame, M. *Inorg. Chem.* **1965**, *4*, 139.

(11) Nakamoto, K. *Infrared and Raman Spectra of Inorganic and Coordination Compounds*, 3rd ed.; Wiley: New York, 1977; Part III, pp 317−324. Adams, D. M. *Metal−Ligand and Related Vibrations;* Edward Arnold: London, 1967; p 277 and references therein.

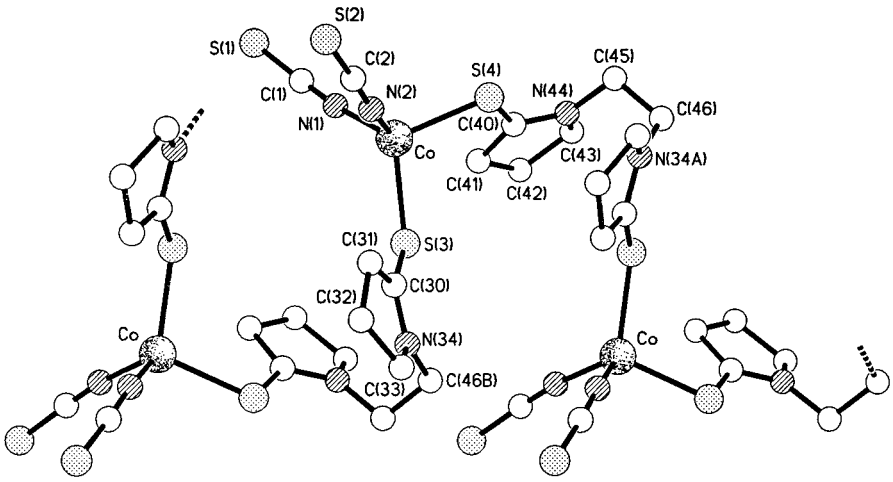

Figure 3. Part of the polymeric chain structure formed by **3**.

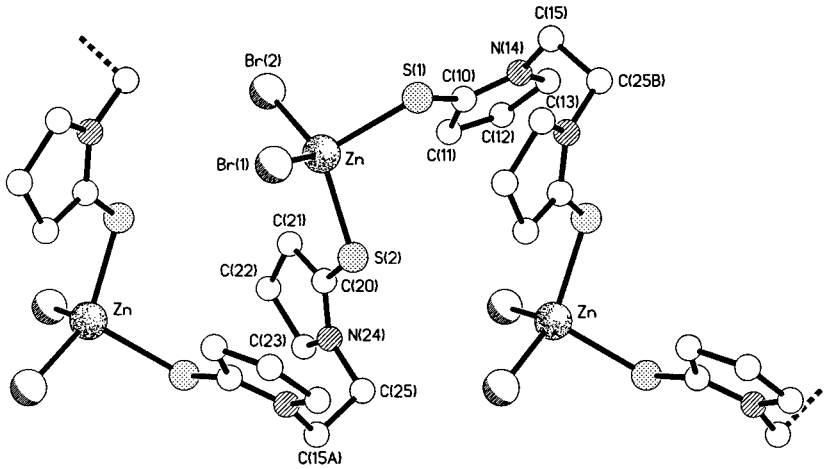

Figure 4. Part of the polymeric chain structure formed by **4**.

bromide the ring has one pair of diametrically opposite S atoms directed inward and lying within the mean plane of the macrocycle (S···S = 4.60 Å), whereas the other pair of S atoms are pseudoaxially directed (S···S = 6.24 Å). However, in $CoCl_2$(EBPT) all four S atoms are directed away from the mean plane of the macrocylic ring (transannular S···S = 6.13 Å). The essential difference is a twist of 180° about one of the N−C(bridge) bonds [N(6A)C(7A) in Figure 2b] which converts the relative orientation of the thiolactam rings from a syn to an anti geometry. The transannular Co···Co distances are, however, largely unaffected (6.89 Å for the chloride and 6.73 Å for the bromide). This change from a syn to an anti geometry is somewhat analogous to that recently reported[12] in some elegant network structures constructed using transoid and cisoid 3,3′-dicyanodiphenylacetylene as a spacer ligand. The macrocycle in **2** is self-filling and is close-packed in the crystal, there being an absence of any significant voids or channels in the lattice.

Structure of $[Co(NCS)_2(EBPT)]_n$ (3). The X-ray study of **3** shows that, as expected from the ν(CN) band at 2056 cm^{-1} in its IR spectrum, the anions are bonded via N (Figure 3). The anions are nearly linear with N−C−S bond angles of 177.5°, and the Co−N−C angles are ca. 168°. The coordination geometry about each cobalt center is again tetrahedral but with much less distortion than in the chloro and bromo complexes; in **3**, with one exception [N(2)−Co−S(3) = 118.9(4)°] all the bond angles at Co are in the range 105.3(4)−109.2(5)°. The Co−S bond lengths (2.32 Å) are essentially the same as those in CoX_2(EBPT) (X = Cl, Br).

In **3**, however, the EBPT ligands bridge adjacent Co centers to form extended chains rather than the rings formed by CoX_2-(EBPT) (X = Cl, Br). The EBPT ligands adopt a "headphones" conformation with the thiolacatam rings in an anti disposition. The torsion angle (NCH_2CH_2N) of the ethylene bridge is 64°, and the C═S vectors of each EBPT unit are inclined to one another at 163°. The chains propagate via the crystallographic *a* glide with an "up−down" arrangement of alternating thiolactam rings; the adjacent cobalt centers within the chain are separated by 6.89 Å.

In the case of $Co(ClO_4)_2(EBPT)_2 \cdot H_2O$, we could not obtain crystals of sufficient quality for X-ray structure determination, but as the solid-state electronic spectrum is typical of a tetrahedral geometry about the cobalt atom, it seems probable that it has a structure analogous to that found for $\{[Co(p\text{-}XBPT)_2](ClO_4)_2 \cdot 4MeNO_2\}_n$ (see later), that is, one in which tetrahedral CoS_4 centers are linked by EBPT bridges to form sheets of contiguous metallacyclic rings (in this case 36-membered rings).

Structure of $[ZnBr_2(EBPT)]_n$ (4). The X-ray study of **4** reveals that the coordination geometry about the metal center is, again, disorted tetrahedral (Figure 4). As in the case of the cobalt analogue, there are only small differences in the Zn−Br and Zn−S bond lengths [Zn−Br(1) = 2.387(2), Zn−Br(2) =

(12) Hirsch, K. A.; Wilson, S. R.; Moore, J. S. *Inorg. Chem.* **1997**, *36*, 2960.

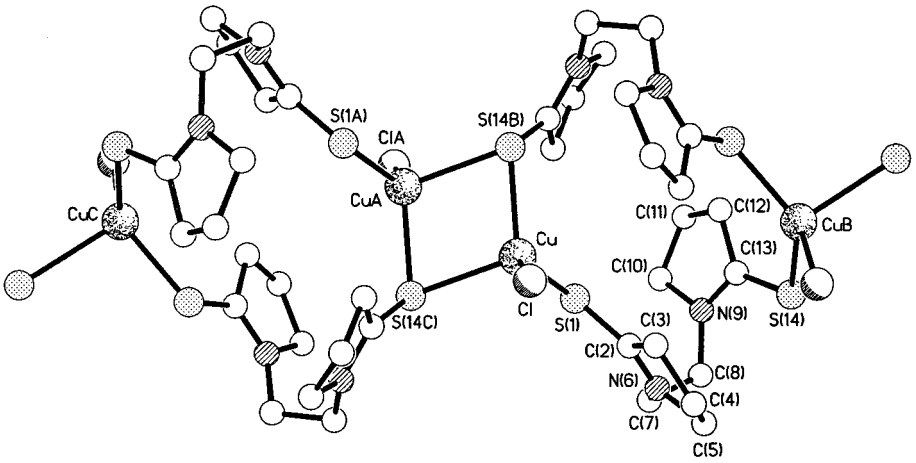

Figure 5. View of part of the linked−ring polymer structure of **5** showing the alternating four- and 18-membered rings.

2.363(2), Zn−S(1) = 2.390(2), and Zn−S(2) = 2.358(3) Å], but the bond angles at Zn [100.9(1)−120.7(1)°] depart significantly from the idealized tetrahedral angle.

The extended structure of **4** is, however, quite different from that of its cobalt analogue as the Zn centers are here linked by the EBPT ligands into chains which propagate via the crystallographic *n* glide. There is, however, a close similarity with the structure of the cobalt isothiocyanate complex **3** discussed above. The EBPT bridges again adopt a "head-phones" conformation; the torsion angle (NCH_2CH_2N) of the ethylene bridge is 68° (cf. 64° in **3**), and the C═S vectors of each EBPT unit are inclined to one another at 157.4°(163.3° in **3**). However, a reversal in the sign of the torsion angle about the Zn−S(2) bond in **4** [S(1)−Zn−S(2)−C(20) = −130°] compared with Co−S(3) in **3** [S(4)−Co−S(3)−C(30) = +117°] results in a change of the overall chain configuration which leads to a shortening of the in-chain M···M separation from 6.89 Å in **3** to 6.12 Å in **4**. It is interesting that such large differences in extended structures (chain or ring) are observed in such closely related sets of compounds in which the metal ion coordination geometries are so similar; we address this point in the conclusions.

The ν(Zn−Cl) and ν(Zn−I) band energies (see Experimental Section) in the vibrational spectra of the compounds ZnX_2(EBPT) [X = Cl, I] indicate that here too the metal ions adopt a tetrahedral coordination geometry, but the samples isolated were unsuitable for X-ray structure determination. This is also the case for the nickel complexes NiX_2(EBPT) [X = Br, I], the electronic spectra of which are characteristic of a distorted tetrahedral metal ion coordination geometry.[10,13] In contrast, the electronic spectrum of the yellow nickel chloride complex of stoichiometry Ni_2Cl_4(EBPT) is typical of six-coordinate nickel,[14] and its IR spectrum has no bands above 200 cm^{-1} assignable to ν(Ni−Cl). Thus it appears that the complex has a structure involving chloride-bridged nickel centers, as in compounds such as Ni(pyridine)$_2$Cl$_2$ or Ni(pyridine)Cl$_2$, but in the absence of crystals suitable for X-ray studies, we cannot determine whether the EBPT ligands act as simple bridges between the Ni atoms or whether each sulfur atom serves as a μ_2 bridge (as in compound **5**, below) and thus generates a more complex polymer.

Reactions of EBPT with copper(II) chloride and bromide in organic solvents caused reduction to copper(I). In the case of the chloride, it was possible to adjust the reaction conditions to permit the isolation of a deep purple Cu(II) complex of the type $CuCl_2$(EBPT).

In the solid state the electronic spectrum of this compound has bands at 9300, 11 800 and 17 900 cm^{-1} and a well-defined three *g* value X-band EPR spectrum. Although these data are insufficient to reliably define the coordination geometry about the Cu center, the EPR observations appear to rule out the presence of either chloride or μ_2-S bridges.

Concentration of the filtrate from the synthesis of $CuCl_2$-(EBPT) gave good crystals of a bright yellow copper(I) complex CuCl(EBPT), the structure of which was determined by X-ray methods.

Structure of [CuCl(EBPT)]$_n$ (5). The X-ray study shows that **5** forms ribbons of alternating four- and 18-membered rings (Figure 5) in which the sulfur donor atoms of each EBPT ligand employ different bonding modes to copper. The C_i symmetric four-membered rings arise from the linking of pairs of copper atoms by the μ_2-S bridging action of a sulfur atom from each of two different EBPT ligands. The other sulfur atom of each EBPT molecule binds in terminal fashion to a copper atom of a neighboring $Cu_2(\mu_2\text{-}S)_2$ unit, thus generating the 18-membered C_2 symmetric rings. The EBPT ligand again adopts a characteristic "headphones" conformation with gauche geometry (70°) about the linking C−C bond and with the C═S bonds in an anti (154°) relationship.

The coordination sphere about each copper atom is completed by a terminal chlorine producing a distorted tetrahedral geometry about each metal center; the interbond angles at Cu are in the range 97.7−124.7°. The four-membered Cu_2S_2 ring has asymmetric Cu−S bond distances of 2.376(1) and 2.593(1) Å. The Cu···Cu and S···S distances within the four-membered ring are 3.01 and 3.69 Å, respectively, with angles subtended at S and Cu of 74.3° and 105.7°, respectively. Within the 18-membered ring, the transannular S···S distances are 4.91 and 7.35 Å, respectively, with the larger separation being that between the pair of μ_2-S bridging sulfurs.

Structure of {[CuBr(EBPT)]·MeNO$_2$}$_n$ (6). The reaction between EBPT and copper(II) bromide in methanol/nitromethane directly gave brown-yellow crystals of a copper(I) complex (**6**) without any apparent formation of a solid copper(II) bromide compound.

The X-ray study of **6** shows that it also forms chains of alternating four- and 18-membered rings based on tetrahedral, dinuclear Cu_2X_2 linking motifs (Figure 6), though this is achieved in a very different way than in the structure of [CuCl-(EBPT)]$_n$. In **6**, pairs of copper atoms are linked by two

(13) Cotton, F. A.; Faut, O. D.; Goodgame, D. M. L. *J. Am. Chem. Soc.* **1961**, *83*, 344.
(14) Lever, A. B. P. *Inorganic Electronic Spectroscopy*, 2nd ed.; Elsevier: Amsterdam, 1984; pp 511−519 and references therein.

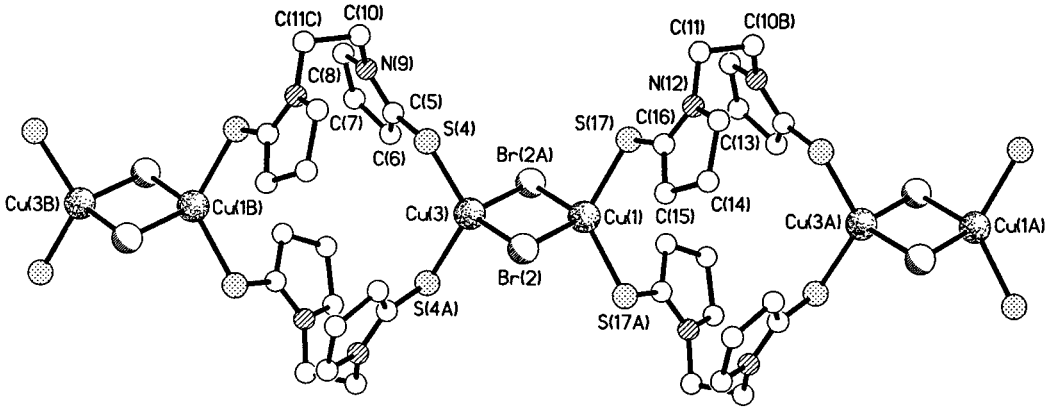

Figure 6. View of part of the linked-ring polymer structure of **6** showing the alternating 18-membered $Cu_2(EBPT)_2$ and four-membered Cu_2Br_2 rings.

bridging bromine atoms so as to form (Cu_2Br_2) units. Each copper atom is also bonded to two terminal sulfur atoms, one from each of two different EBPT ligands, which, in turn, bridge adjacent Cu_2Br_2 units to form chains of 18-membered $Cu_2(EBPT)_2$ rings. In this structure both the four- and 18-membered rings have C_2 symmetry about an axis passing through the copper atoms. Despite the differences in the nature of the bridging atoms, the range of interbond angles at Cu in **6** (97.1−123.9°) is virtually the same as that in **5.** Within the Cu_2Br_2 ring the Cu···Cu and Br···Br separations are 2.90 and 4.24 Å, respectively.

The $Cu_2(EBPT)_2$ rings in **6** have a conformation similar to that in $[CoCl_2(EBPT)]_2$. The thiolactam rings of each EBPT in **6** have an anti conformation with C═S vectors at 158.1° and a gauche arrangement around the ethylene bridge, with a torsion angle (NCH_2CH_2N) of 65.4°. The sulfur atoms are directed up and out of the mean plane of the $Cu_2(EBPT)_2$ ring and have a transannular S···S separation of 6.31 Å. The occluded nitromethane molecules of solvation lie between the chains.

It is interesting to compare the anion dependence of the structures of the three copper(I) complexes: $[CuCl(EBPT)]_n$ (**5**), $[CuBr(EBPT)]_n$ (**6**), and $\{[Cu(EBPT)_2](PF_6)\}_n$.[6a] In each case, chains of 18-membered $Cu_2(EBPT)_2$ rings are formed with the rings linked by units involving tetrahedrally coordinated Cu centers, but the nature of those connecting units differs appreciably. In $\{[Cu(EBPT)_2](PF_6)\}_n$, where the anion has a very poor coordinating ability, each copper(I) center comprises a simple tetrahedral CuS_4 unit, resulting in chains of spiro-linked 18-membered $Cu_2(EBPT)_2$ rings. In **6** the bromine atoms link pairs of copper atoms, thus forming Cu_2Br_2 units which then serve to connect $Cu_2(EBPT)_2$ rings into chains.

In **5** the dinuclear Cu units which connect the $Cu_2(EBPT)_2$ rings are produced by pairs of μ_2-S bridges from the EBPT ligands, and the Cl anion is simply bonded to copper in terminal fashion.

What is less obvious is the reason for the difference between the chloride and the bromide, as a bridging role for chloride ions between copper(I) is very well-established. We do not think it unreasonable to conclude that, as there appear to be no steric constraints imposed by the halogen atoms, the two structure types observed for **5** and **6** represent equally probable minimum energy structures and are not per se halogen-dependent, and the isolation of a given form may depend simply on the experimental conditions prevailing during crystallization. Inspection of the packing did not reveal any obvious anion-dependent intermolecular interactions.

From a reaction between hydrated copper(II) perchlorate and EBPT, we also isolated a yellow complex which, from microanalytical results, had the composition $Cu(ClO_4)$(EBPT), but the product was unsuitable for X-ray characterization.

Complexes of *N,N′-p*-Phenylenedimethylenebis(pyrrolidine-2-thione). As other extended-reach ligands with the *p*-phenylenedimethylene linking unit, but employing N or O donor atoms, have given examples of interwoven structures,[1a,5,15,16] it was of interest to investigate whether such interweaving might also be adopted by ligand **III** (*p*-XBPT), which contains the *p*-phenylenedimethylene spacer group. With the metal salts we have studied, the complexes formed by *p*-XBPT are generally similar to those with EBPT in terms of their stoichiometries and coordination geometries at the metal centers, for example, tetrahedral coordination at the metal centers in CoX_2(*p*-XBPT) [X = Cl, Br, I] and in NiX_2(*p*-XBPT) [X = Br, I]. It was, however, more difficult to obtain crystals suitable for X-ray determination of their extended structures because the compounds have poorer solubility in common organic solvents and some tended to form oils on attempted crystallization. In two cases, $Ni(NO_3)_2$(*p*-XBPT) and $[Co(p\text{-XBPT})_2](ClO_4)_2\cdot 4MeNO_2$, X-ray structural analysis was possible, and the results extend the range of structural types described above for the EBPT compounds.

Structure of $[Ni(NO_3)_2(p\text{-XBPT})]_n$ (7). The solid-state electronic spectrum of **7** [8500 $^3A_{2g} \rightarrow {}^3T_{2g}$, 14 700 $^3A_{2g} \rightarrow {}^3T_{1g}$(F), 23 300 $^3A_{2g} \rightarrow {}^3T_{1g}$(P) cm^{-1}] shows that the nickel is six-coordinate. The X-ray study reveals that this is a distorted C_2 symmetric *cis*-NiO_4S_2 coordination sphere comprising two equivalent nitrate groups bonded in slightly asymmetric chelating fashion (Ni−O 2.07 and 2.13 Å) and two cis-disposed sulfur atoms, one from each of two different *p*-XBPT ligands (Ni−S = 2.37 Å) (Figure 7). The C_i symmetric *p*-XBPT ligands bridge the nickel centers so as to form chains. The *p*-XBPT ligand has a chair conformation and an anti disposition of its C═S groups. There are no significant interchain interactions other than normal van der Waals interactions.

The cis octahedral NiO_4S_2 coordination geometry in **7** appears to be rare, a search of the Cambridge Crystallographic Database revealing only one other example of a *cis*-$M^{II}(NO_3)_2S_2$ system, viz., $Co(NO_3)_2[(Me_2N)_2CS]_2$.[17] In that cobalt complex the nitrate groups are bound in a more asymmetric fashion (Co−O 2.017, 2.377 Å and 2.036, 2.490 Å; cf. 2.073, 2.130 Å in **7**). In both compounds, however, the longer M−O distances are associated with the oxygen atoms trans to the sulfur atoms.

(15) Goodgame, D. M. L.; Menzer, S.; Smith, A. M.; Williams, D. J. *Angew. Chem., Int. Ed. Eng.* **1995**, *34*, 574.
(16) Goodgame, D. M. L.; Menzer, S.; Smith, A. M.; Williams, D. J. *J. Chem. Soc., Chem. Commun.* **1995**, 1975.
(17) Pignedoli, A.; Peyronel, G. *Acta Crystallogr.* **1978**, *B34*, 1477.

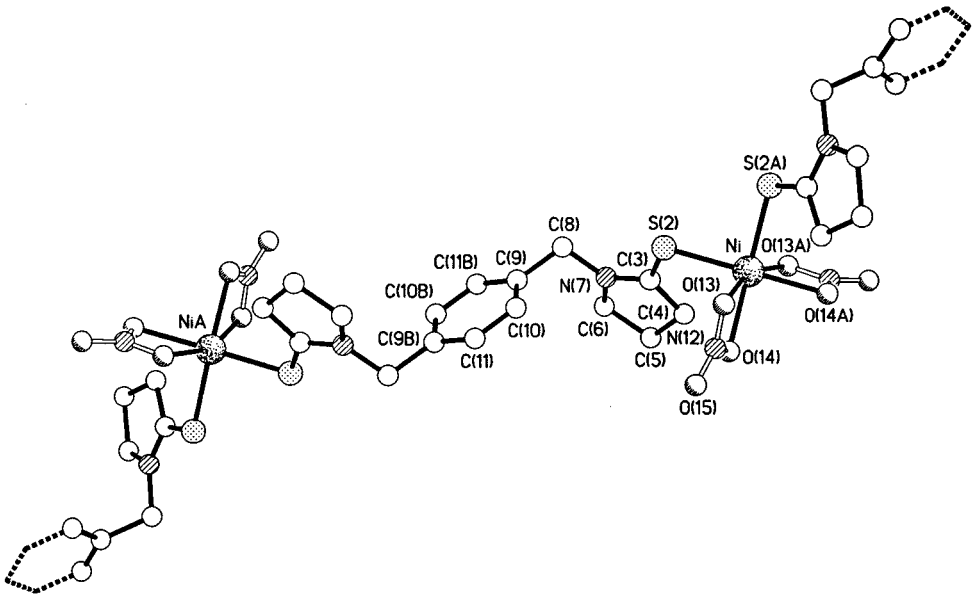

Figure 7. Part of the polymeric chain structure formed by **7**.

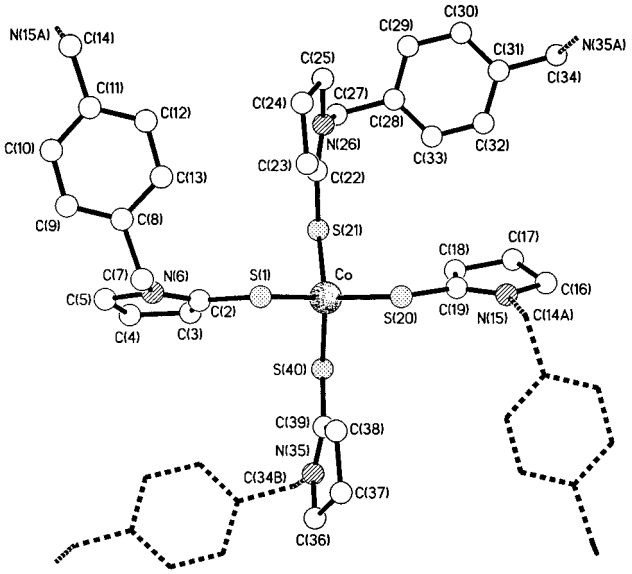

Figure 8. The cobalt coordination environment in compound **8**.

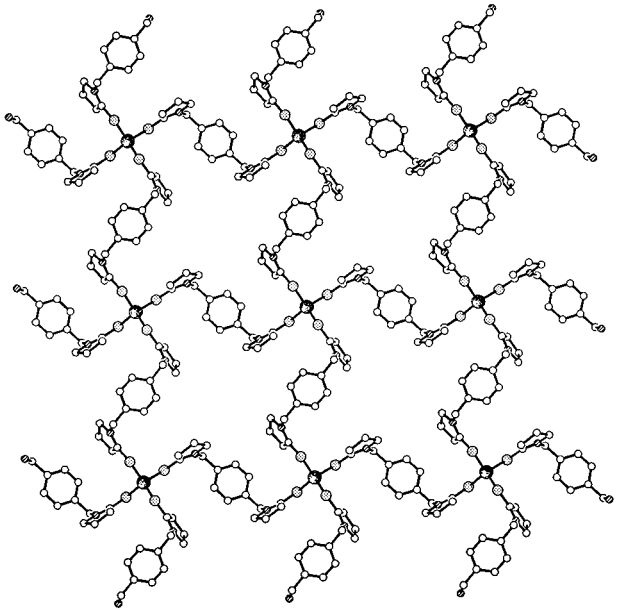

Figure 9. Part of one of the sheets of contiguous 52-membered rings in the structure of **8**.

Structure of $\{[Co(p\text{-}XBPT)_2](ClO_4)_2 \cdot 4MeNO_2\}_n$ (8). The solid-state electronic spectrum of this green compound (see Experimental section) indicates the presence of a tetrahedral coordination geometry. The X-ray study confirmed that this is the case; each cobalt atom is bonded to four sulfur atoms, one from each of four *p*-XBPT ligands (Figure 8). The CoS_4 tetrahedron is not completely regular; the bond angles at Co are in the range 96.0−117.9°, but the differences in the Co−S bond distances are relatively small (2.31−2.34 Å).

The bridging action of the *p*-XBPT ligands generates sheets of contiguous 52-membered rings propagated within the crystallographic 110 plane (Figure 9). Within each ring there are two crystallographically different pairs of *p*-XBPT ligands; their conformations, however, are very similar and, indeed, the macrocycle has approximate S_4 symmetry. The thiolactam units adopt a near-eclipsed arrangement, with torsion angles of 14° between N(6)−C(7) and C(14)−N(15A) and 18° between N(26)−C(27) and C(34)−N(35A), respectively, resulting in a "horseshoe" conformation. The C═S vectors in the two independent ligands are anti-disposed (61° and 65°).

The sheets, which are distinctly corrugated, are stacked so that the phenylene rings are aligned approximately parallel, but in offset fashion (Figure 10). Adjacent sheets are arranged in an "up−up"/"down−down" sequence along the crystallographic *c* direction and produce channels which in one direction are between "up" and "down" pairs (as indicated in Figure 10), and orthogonally so that there are channels between "down" and "up" pairs. These channels, which do not intersect, contain the perchlorate anions, which are disordered, and the included nitromethane molecules of solvation. Unprotected crystals rapidly lose their solvent molecules after removal from their mother liquor, and air- or vacuum-dried bulk samples had analyses corresponding to the solvent-free formulation, $[Co(p\text{-}XBPT)_2](ClO_4)_2$.

As stated earlier, it seems likely that the complex $Co(ClO_4)_2(EBPT)_2 \cdot H_2O$ has a structure similar to that of **8**, but with a reduction in ring size from 52-membered to 36-membered.

Reactions of *p*-XBPT with silver perchlorate and silver tetrafluoroborate, respectively, gave the compounds $Ag_2X_2(p\text{-}$

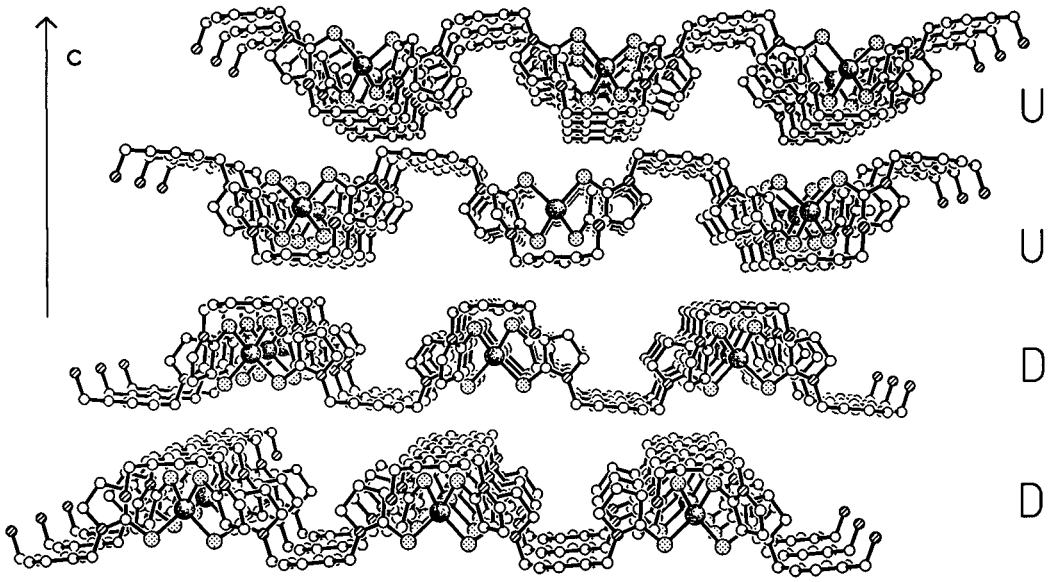

Figure 10. Stacking of adjacent sheets in the structure of **8**, showing some of the channels created by the "up" (U) and "down" (D) sheet orientations.

Table 10. Comparison of Selected Structural Features for Compounds **2**−**6**, $[CoBr_2((EBPT)]\cdot 1.5MeOH$,[6a,18] and $\{[Cu(EBPT)_2](PF_6)\}_n$[6a,18]

compd	EBPT conformation	C=S vector (deg)	N−CH_2−CH_2−N[a] (deg)	ring/ chain
2	anti	157	67	ring
$CoBr_2$(EBPT)	syn	65	68	ring
3	anti	163	64	chain
4	anti	157	68	chain
5	anti	154	70	ring
6	anti	158	65	ring
$[Cu(EBPT)_2](PF_6)$	syn	61, 68[b]	64, 70[b]	ring[b]

[a] Gauche. [b] The structure of $[Cu(EBPT)_2](PF_6)$ contains two sets of $Cu_2(EBPT)_2$ rings.

$XBPT)_3\cdot H_2O$ (X = ClO_4, BF_4). The observed stoichiometry points to the formation of a network structure, and it is tempting to postulate that interweaving may be involved [cf. the "polyrotaxane" network recently reported[1a] for $\{[Ag_2(bix)_3](NO_3)\}_n$, where bix = $N_1N'_1$-*p*-phenylenedimethylenebis(imidazole)]. However, the μ_2-bridging potential of the sulfur donor atoms in *p*-XBPT (as in **5**) could vitiate such straightforward comparison, and we were unable to obtain crystals of these compounds to explore this possibility.

Conclusions. Within the inevitable constraints of the availability of compounds of suitable crystallinity, the X-ray structural results described here show that, for the metal ions studied, the bis(thiolactam) ligands resemble their O-donor analogues in their general ability to generate polymeric structures comprising individual large rings, chains and sheets. The types of extended structures that are produced arise partly from the preferred coordination geometry at the metal centers and partly from the conformational properties available to these "extended-reach" ligands. Notwithstanding the large differences in the various types of long-range structure, there are notable consistencies in the ligand conformations (Table 10), and it appears that it is the way these are employed that generates the particular structure adopted.

The key to the use of extended-reach ligands in the design of dimensioned network architectures is the ability to control both metal coordination and ligand geometries. Within the series of structures discussed here it can be seen that although some of these parameters have exhibited the desired degree of control, namely type of metal coordination and a consistency of a gauche relationship between the two thiolactam units, it is clearly evident that the ability of the two sulfur donor groups to "flip" between syn and anti relationships has a major controlling influence. This change, which might appear to be comparatively minor in the context of the total number of variable geometric parameters, leads to the formation of a diverse range of structural types, such as the chains or discrete rings observed here. The obvious lesson to be learned is that, although one can still capitalize upon "electronically preferred" conformations of extended-reach ligands to design network structures, additional steric constraints may have to be incorporated to achieve an appropriate level of control.

The present work does, however, suggest some specific differences between the bis(lactams) and their thio analogues. The reducing power observed in the formation of Cu(I) complexes from Cu(II) precursors has no parallel in our results with the lactam ligands, and this points to possible exploitation in forming further types of networks with other metal ions in their lower oxidation states. The formation of μ_2-S bridges in **5** is an additional feature that may prove to be more important with the thio ligands than with their O-donor analogues, especially with "soft" metal ions. Finally, reactions of **I** and **III** with metal salts of essentially noncoordinating anions (e.g., ClO_4^- or BF_4^-) gave[18] no examples of compounds of the type $[ML_3]X_2$ with an octahedral MS_6 coordination sphere analogous to the octahedral ZnO_6 coordination found[4a] in the compound $[Zn(ebpyrr)_3](ClO_4)_2\cdot 2MeCN$ formed by the lactam analogue of **I**. This difference may reflect increased steric constraints in the case of the thiolactam ligands, at least for the sizes of the metal ions we have studied.

Acknowledgment. We thank the EPSRC for a Research Studentship (to Z.A.), for a postdoctoral fellowship (to S.M.), and for the diffractometers.

Supporting Information Available: Tables giving details of the crystallographic data collection and structure refinement, atomic coordinates and equivalent isotropic thermal parameters, a full set of bond lengths and angles, anisotropic displacement coefficients, and H atom coordinates and displacement coefficients (48 pages). Ordering information is given on any current masthead page.

IC971180P

(18) Atherton, Z. Ph.D. Thesis, London University, 1996.